A MODEL OF LAGGING FRICTION AS A FUNCTION OF CREEP HISTORY AND WRAP PRESSURE

B DeVries
Flexible Steel Lacing Company

INTRODUCTION

Lagging friction is a topic of ongoing discussion and analysis. Conservative values for friction coefficient have been used for years in the design of drive systems yet fall short when unexpected wear patterns arise, or compound drive oscillations occur. Clearly a better model of the underlying mechanisms that give rise to instantaneous friction level would be valuable towards better conveyor design and operation. This paper describes and mathematically models two of these mechanisms to create a holistic view of frictional driving a conveyor belt.

BACKGROUND

In the earlier "Variants" paper, evidence was provided for the dependence of lagging friction on wrap pressure. It was also noted that the tested lagging did not exhibit a classic static and dynamic friction coefficient, but instead progressively increased with further displacement. In that paper 6.35 mm of travel was used as a comparison point. Upon review, justification for this value appeared incomplete. A more rigorous description of lagging friction behaviour in response to slip distance remained unexplored.

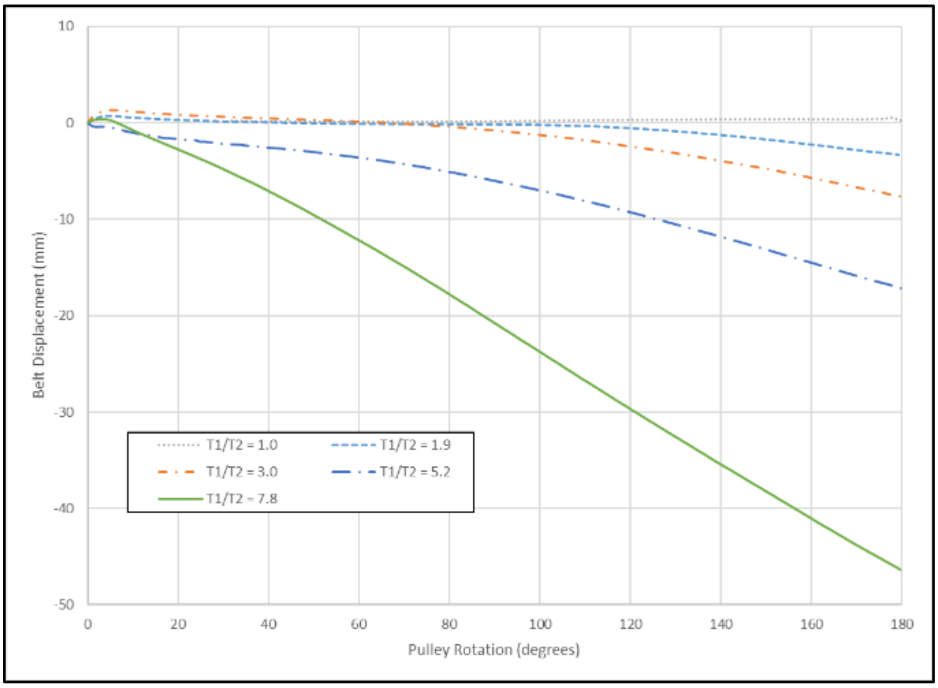

Figure 1 – Belt displacement vs pulley wrap angle for increasing tension ratios. Belt wworking strength: 175 kN/m.

For real world pulleys, it is difficult to obtain data on belt creep, especially under multiple loading scenarios. Conveyors are designed with specific tension ratios for operation and cannot realisticaly be adjusted. It is also difficult to obtain a window to affix measurement sensors to a pulley since sites like to keep them operating. As a result lab data and computer simulations are relied on for data. For example, lab data for belt displacement was reported in “Surface Dynamics”. The data shows that displacement is influenced by the increasing tension ratio. Observe the largest ratio is slipping throughout the wrapped arc. As the tension ratio demands increase, the result is increasingly greater relative movements between the belt and lagging. This is not break-away slip but merely a gradual creep. Since increased tension ratios require greater friction coefficients to sustain, it seems logical to suspect that the greater relative movements between the lagging and belt may be driving increasing friction coefficients.

TESTING

To begin the investigation, friction data from three lagging samples was re-examined. They are identified as Diamond rubber, Medium Ceramic, and Full ceramic, see Figure 2. All three samples were approximately 200 mm square.

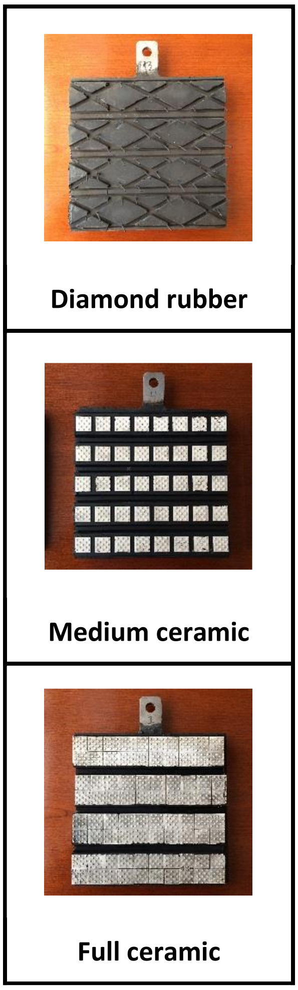

Figure 2. Lagging test samples

The Diamond rubber sample is composed of a proprietary SBR/BR rubber compound with a diamond shaped tread pattern moulded therein and is 12 mm thick.

The Medium ceramic sample contained evenly spaced 20mm ceramic tiles with raised nubs. Each tile is embedded and bonded to an SBR/BR rubber matrix. The tile and rubber together take the form of a raised projection with the nubs of the tile extending 1mm above the common surface of the tiles and rubber. A 10mm wide channel runs between each row for contamination egress. The overall thickness of the lagging is 15 mm. The tiles comprise forty per cent of the total surface area.

The Full ceramic sample is comprised of the same 20mm ceramic tiles arranged tightly adjacent such that the entire surface presented to the belt is only tiles. Water channels run between every two rows of tiles resulting in total contact area being 80% ceramic tile and 20% voids. The overall thickness of the sample is 12 mm.

Each lagging type was glued to both sides of a steel plate to create a test sample. Each sample was then sandwiched between pieces of conveyor belt, which were affixed to clamping plates. The clamping plates evenly applied normal force to the belt and lagging interface. The normal force F_n was measured with a load cell. Once clamped, the lagging sample was extracted from between the belt samples by pulling on the steel plate with a tensile test machine. The extraction force F_x was measured and plotted as a function of crosshead movement in the tensile test machine. Likewise, the instantaneous coefficient of friction, μ, is easily calculated with equation 1 and may be plotted as a function crosshead movement.

$$\mu = \frac{F_x}{2F_n} \qquad 1$$

RESULTS

Figures 3, 4, and 5 show the consolidated plots of the friction coefficient vs. crosshead displacement. The figures clearly illustrate decreasing friction coefficient as the test pressure increases. It is also clear that slip distance is an important factor that needs to be included in analysis to obtain accurate values for friction coefficient. The offset in the zero point on some of the larger pressure curves is a result of lash in the test apparatus and should be ignored.

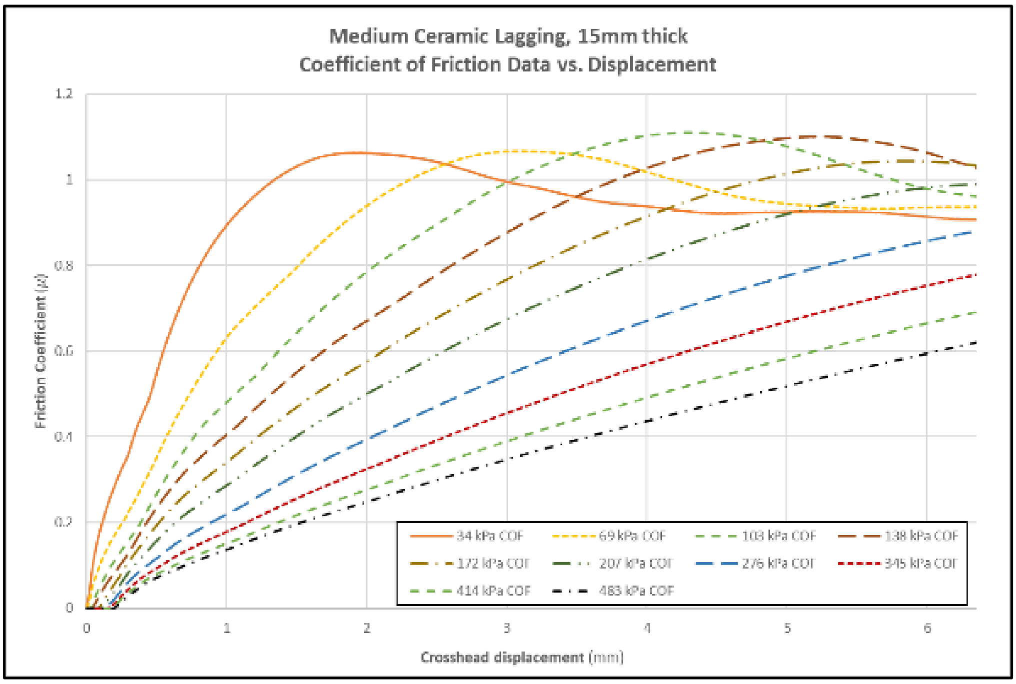

Figure 3 – Consolidated plot of Diamond rubber friction curves

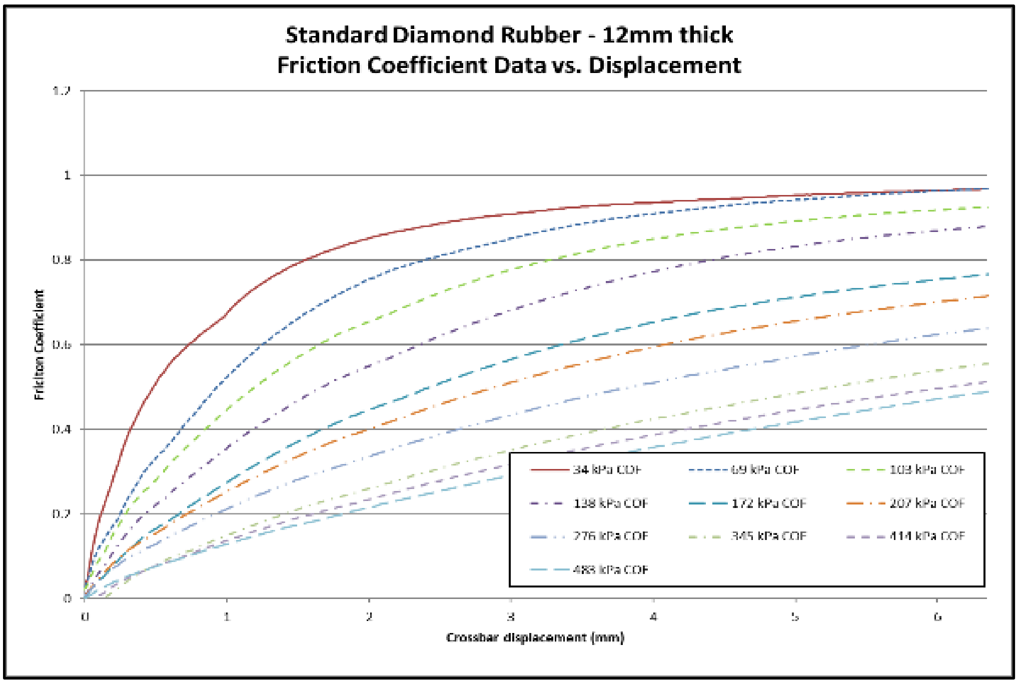

Figure 4 – Consolidated plot of Medium ceramic friction curves.

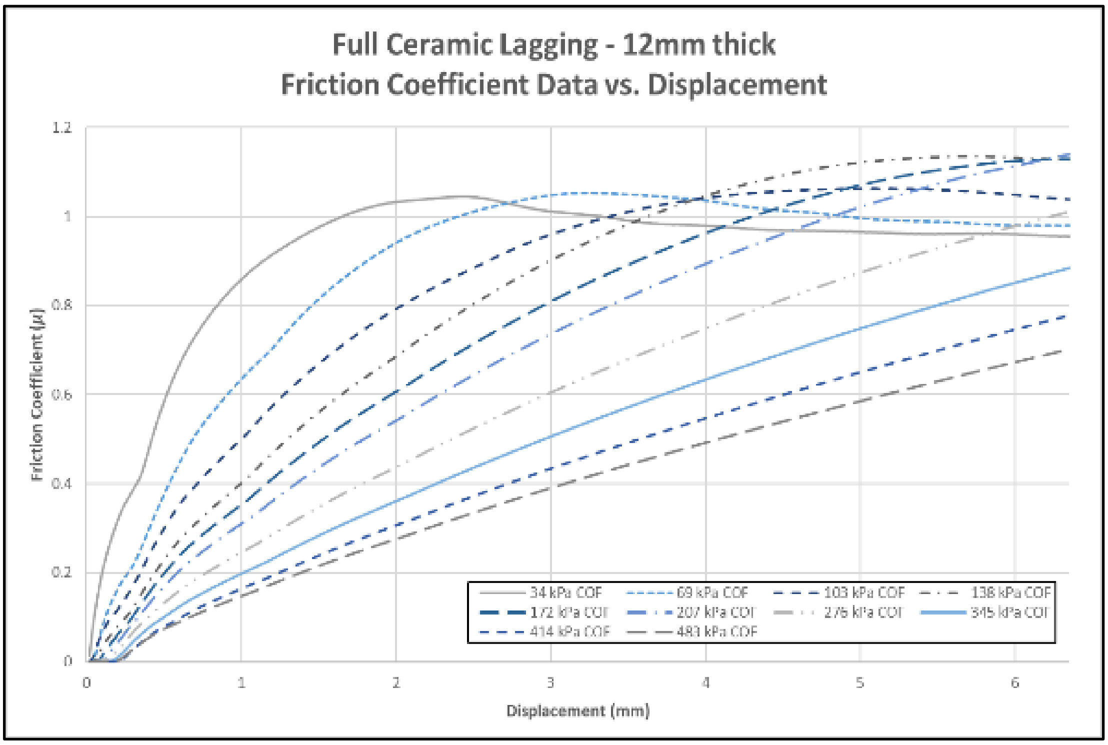

Figure 5 – Consolidated plot of Full ceramic friction curves.

Perrson has studied the effect of temperature on rubber friction in tyres. His theory is that friction is increased by increasing internal energy in the bulk rubber, which is supported by Figures 3, 4, & 5.

Another feature worth noting is the ceramic low-pressure tests clearly exhibit a static and dynamic coefficient of friction. The peak friction coefficient moves towards larger slip distances as the pressure increases until it disappears at 172 kPa.

ANALYSIS

So, what can be done with these plots? Conveniently, a 5-point numerical differentiation of the Diamond rubber 207 kPa curve was easily fit by a natural logarithmic curve. Therefore, the obvious choice to model these curves would be the integral of natural logarithm,

$$\mu = Axln(x) - bx \qquad 2$$

where *A* and *b* are curve fit constants of each pressure data set and lagging type, and *x* is the displacement value. This curve fit equation also nicely fit the Medium ceramic and Full ceramic data sets, despite the change of material for the friction surface and the protruding ceramic nubs. However, a challenge arose with the low-pressure data sets.

At low pressures the macro scale of the ceramic lagging behaved somewhat classically due to the incomplete indentation of the nubs into the belt surface. It is possible to use this integral log equation as a model of friction as it rises to the peak friction value, but the data plot diverges from the equation when the friction value levels out post peak. Caution should be applied using the equation for low wrap pressures. After reaching peak value, the equation quickly drops to zero while actual friction remains near the peak value. Ideally, the integral logarithm equation would be used until the peak is reached and then switched to a simple linear approximation for the friction value thereafter.

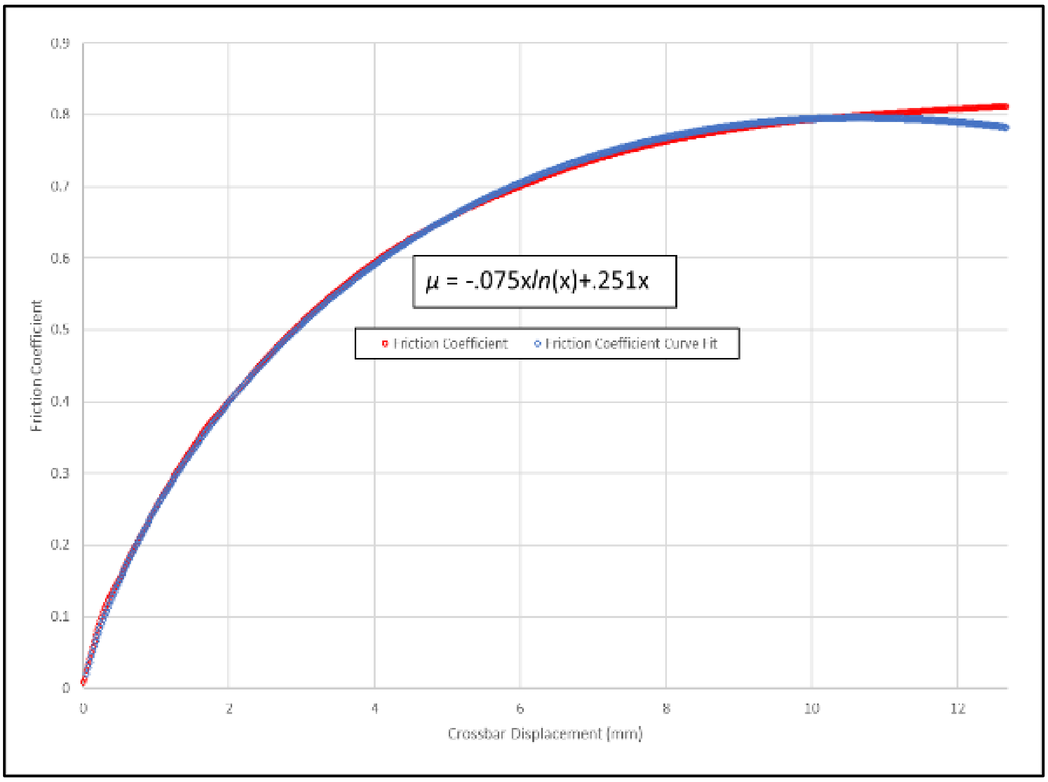

Figure 6 – Comparison of 207 kPa Diamond rubber data to curve fit *Axin(x)-bx* equation

The next challenge was to see if the curve fit constants fell into a rational pattern. If continuous mathematical expressions for the constants could be used to generate the *A* & *b* inputs for the integral logarithmic friction equation, the friction factor could be calculated at any point on the pulley, assuming the wrap pressure and creep history were known at that point. By extension, the traction (shear force) at that point would be computed as the product of friction and pressure. The actual friction coefficient could finally be discretely computed at every point of the entire wrap arc.

Figures 7, 8, and 9 show the results of curve fitting the *A* and *b* coefficients for Diamond rubber, Medium ceramic, and Full ceramic.

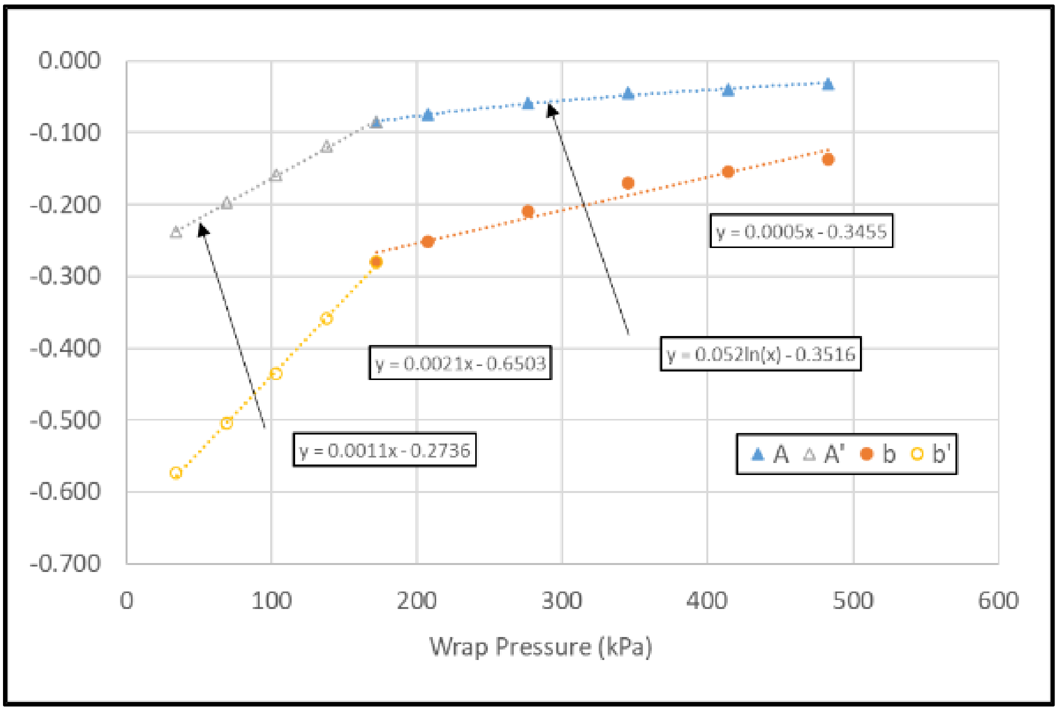

Figure 7 – Diamond rubber friction function coefficients equations

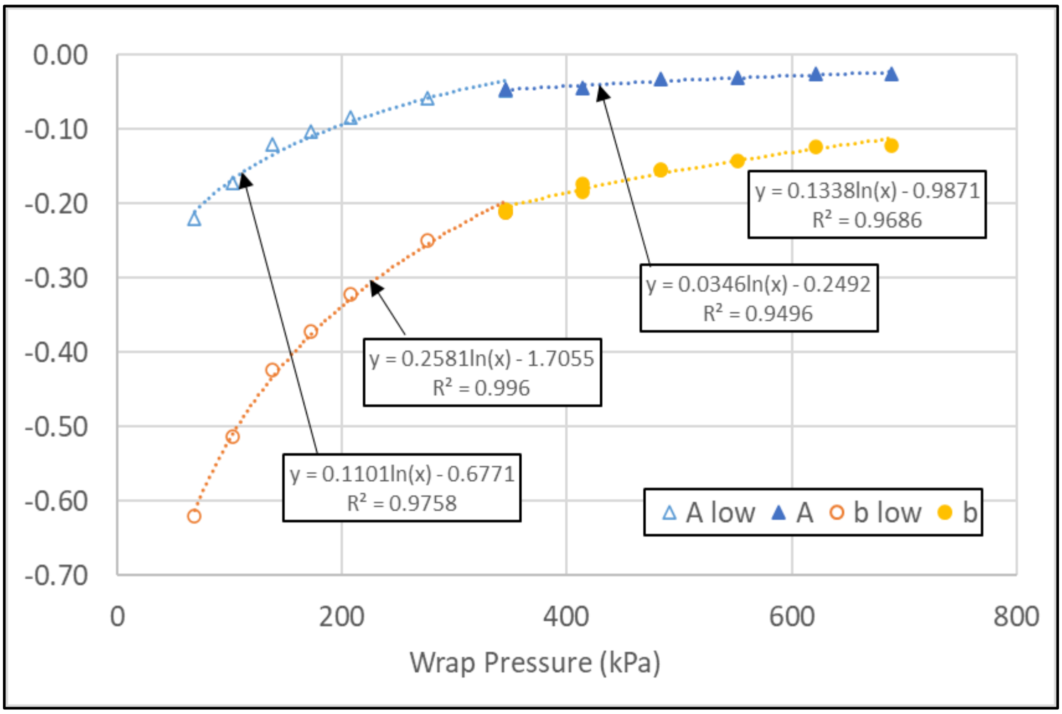

Figure 8 – Medium ceramic friction function coefficients equations.

The transition in the Diamond rubber coefficients at 172 kPa indicates the saturation point of surface contact. Recall Tabor describes friction as the adhesion force occurring in areas of true contact while increasing normal force brings more and more apparent contact area into true contact. Since rubber has a very low elastic modulus, "Variants" proposed that the apparent contact area was saturating to real contact area under typical belt wrap pressures. Inspection of the lagging sample and the belt surface suggests a surface roughness of the lagging and belt to average .3mm, with a lagging thickness of 12mm. The strain required to compress out the surface roughness is

$$.3\ mm/12\ mm = .025. \qquad 3$$

A common value for SBR rubber elastic modulus is 6.9 MPa. Stress is modulus multiplied by strain,

$$6.9\ MPa * .025 = .17\ MPa, \qquad 4$$

which is very near the transition pressure shown in Figure 7. Tabor also explains the near linear nature to the coefficient equations above .17 MPa. Friction at each pressure is increasing with creep in an integral logarithmic fashion, but the change in this function between pressures is linear.

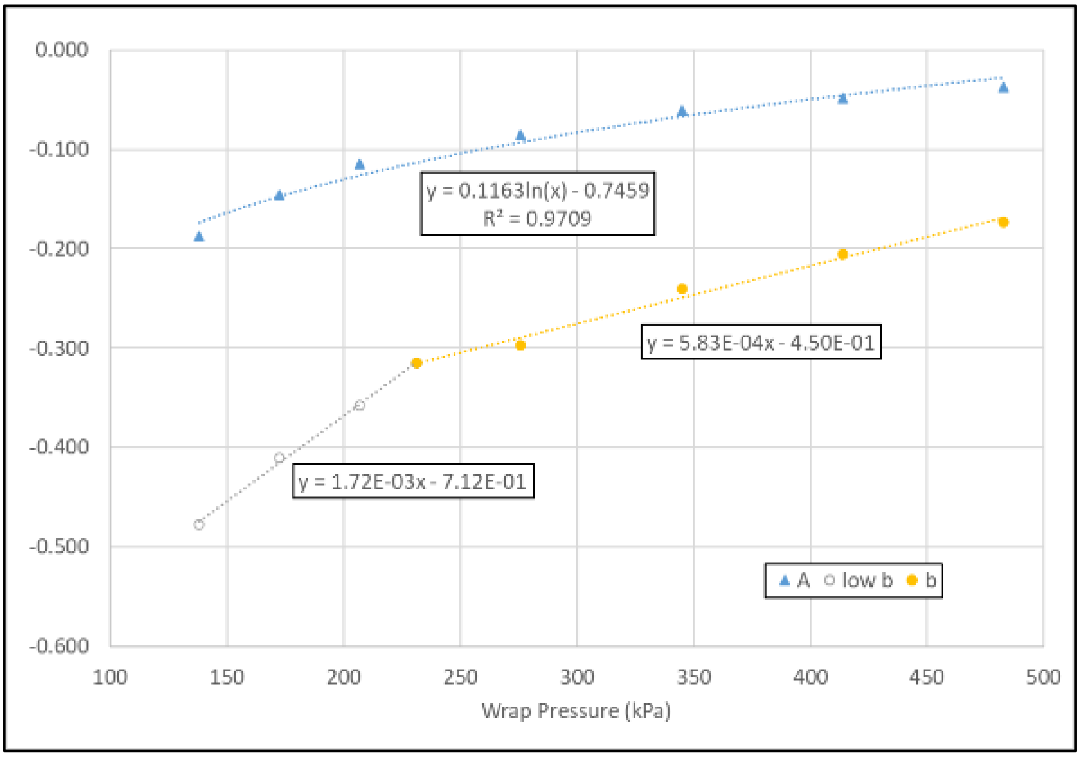

Figure 9 – Full ceramic friction function coefficients equations.

Both the medium and full ceramic plots suggest a transition around 230 kPa. This would be the wrap pressure necessary to fully bed the nubs into the cover of the belt. The greater scatter in the low-pressure coefficients of the medium ceramic coefficients is to be expected given the combination of ceramic and rubber elements in the lagging design. Considering the rubber contact area saturation process is overlaid with the nubs progressively embedding into the belt cover, it is no surprise that the behaviour defies a single mathematical expression. Yet, the curve fit is good enough to be useful.

At this this point the original goal has been realised. Lagging friction behaviour for these three types has been mathematically described based on slip distance and wrap pressure inputs.

Recall "Variants" related wrap pressure and belt tension with the simple expression,

$$T = \frac{pD(BW)}{2} \qquad 5$$

Which can be rearranged,

$$Wrap\ Pressure = \frac{2*Belt\ Tension}{Belt\ Width*Pulley\ Diameter} \qquad 6$$

Equation 6 is true at any scale since it is derived by the static equilibrium of any $d\theta$ of the wrap arc.

A complete model of the tension, pressure, slip, and shear stress for a drive pulley is now possible once the mechanisms of creep can be identified and quantified.

PULLEY CREEP SOURCES

The evidence for belt creep on driven pulleys is abundant. Lagging wear itself is proof since wear will only occur if there is relative movement between the belt and lagging surface.

In many situations aggressive lagging wear is indicative of another conveyor problem. Ultimately, most instances can be attributed to non-uniform tension profiles as the belt enters or traverses the pulley. This analysis seeks to understand the wear mechanisms encounter by a properly engineered and maintained conveyor. Here, the principal mechanism for creep is belt shrinkage due to tension removal. The amount of shrinkage will be directly related to the spring rate of the belt or k factor, which is easily calculated. Belt manufacturers publish a modulus of the belt in units of force per unit width. This is a theoretical force that would double the length of any given length of belt. To transform this modulus into a k factor, some length of belt must be assumed that is either stretching or shrinking to act as a "spring". This length of belt will be the active arc. The active arc is the portion of the wrap arc where the tension is being substantially removed from the belt.

With belt modulus and an assumed length, the k factor of the belt may be calculated.

$$k = \frac{(belt\ modulus*belt\ width)}{active\ arc\ length} \qquad 7$$

The magnitude of belt shrinkage is $\Delta T/k$. This shrinkage will usually be a principal source of the creep that generates the friction coefficient to drive the belt.

A second mechanism for belt creep is lagging compressibility. When the belt first contacts the pulley, the lagging is uncompressed. As the lagging receives the wrap pressure, it will compress and bulge out into void areas. This compression results in an overall smaller diameter than when the belt was first received causing a small belt overrun in the direction of belt travel. Evidence of this can be seen in the brief positive spikes in the belt movement from “Surface Dynamics”. See Figure 11. This is usually a small amount of creep, but since it happens at the entry nip point, it kicks off the friction function to non-zero friction right away.

A third mechanism for belt creep is global creep. This occurs when the tension difference between T1 & T2 is greater than what can be sustained by the friction generated by the first two mechanisms. Figures 3, 4, & 5 clearly show that additional slip will generate high friction coefficients, so the belt begins backsliding until the tension difference is sustained. Global creep is a common feature in drives of high modulus belts because the tension change in the active arc results in little belt shrinkage. In most ply belts, however, global slip is usually a good indicator that too much tension change is being demanded and excessive wear will result.

These mechanisms combine to allow for a creep history model of drive pulley lagging friction. But what creep distance is acceptable? A conservative value for total creep is 6.35 mm, but higher values may be necessary or tolerated for steel cord belts rated higher than ST1600 or fabric belts with working tension above 140 kN/m.

APPLICATION

A calculator may be constructed using the three creep mechanisms and the wrap pressure/creep history friction functions.

1. Divide the wrapped length of the pulley into many smaller segments approximately 2.5mm in length.
2. Start at the exit point of the pulley. At this point all the creep mechanisms are at their maximum. Initial wrap pressure is calculated using the T2 tension. Assume the active arc is equal to the wrapped arc for now. Begin by calculating A & b coefficients based on T2 pressure. Select a desired belt creep. A good guess is to assume the entire wrap arc is your belt length to calculate k factor, and the desired ΔT/k is the creep. This creep should be used in the initial *Axln(x)-bx* to calculate the starting friction coefficient at the exit nip point. Next, calculate a traction increment by multiplying friction by pressure and segment length. The belt is driven by the sum of all the traction increments of the wrap arc.
3. Add the traction increment to the previous tension. Repeat the calculations in step three but be sure to deduct a segment length from the active arc length. This will reduce the slip used to calculate friction. It is also necessary to calculate the shear angle of the lagging and deduct this distance from the creep distance. In general, friction will drop, and pressure will increase as the calculations move to the entry nip point.

Following these steps an iterative calculator was constructed. It was compared to sensor data obtained for “Surface Dynamics”. The calculator incorporates new parameters to calculate lagging friction behaviour, but the results now resemble the measured data much more authentically than existing lagging friction models. Note that the calculator predicts -2.86° maximum shear and -11.8 mm (-.463 inches) creep Figure 10. The test pulley data showed -2.86° maximum shear and -13.0 mm (-.513 inches) of creep Figure 11.

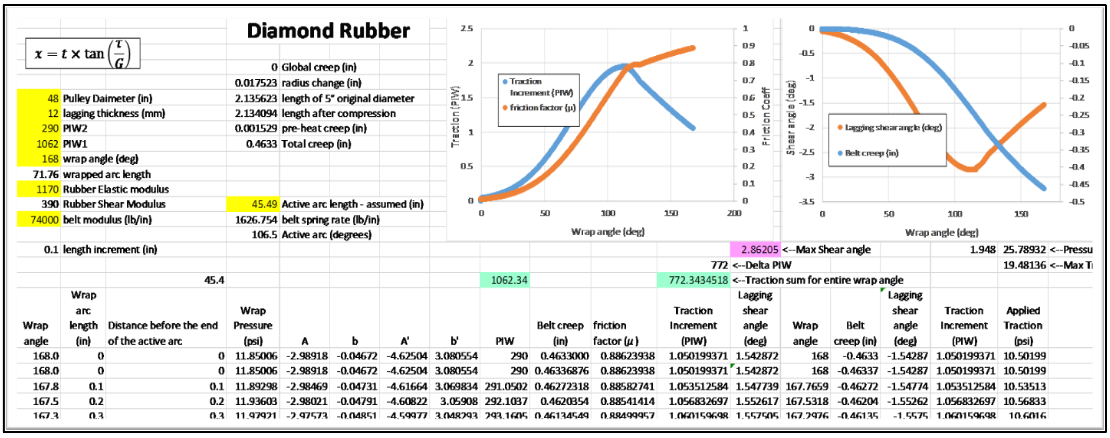

Figure 10 – Screenshot of lagging calculator with inputs matching lagging test pulley

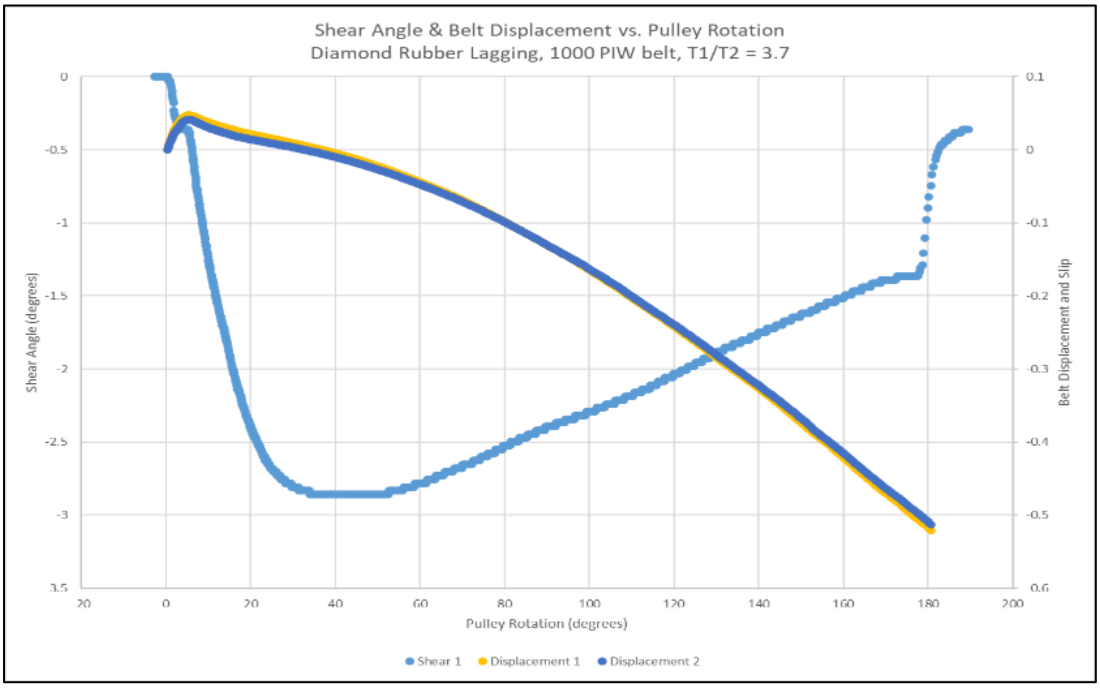

Figure 11 – Plot of belt displacement and lagging shear angle data as a function of pulley rotation angle. Data captured while pulley is rotating.

Multi drive conveyors with load sharing pulleys can also benefit for this calculator. New drive technologies can precisely synchronise drive speeds. The calculator has predicted that second drives in a tandem drive may need to go slightly faster to compensate for greater lagging slips needed to provide the same torque as the first drive. This is a non-intuitive prediction, but it explains tandem drive issues seen in industry Figure 12.

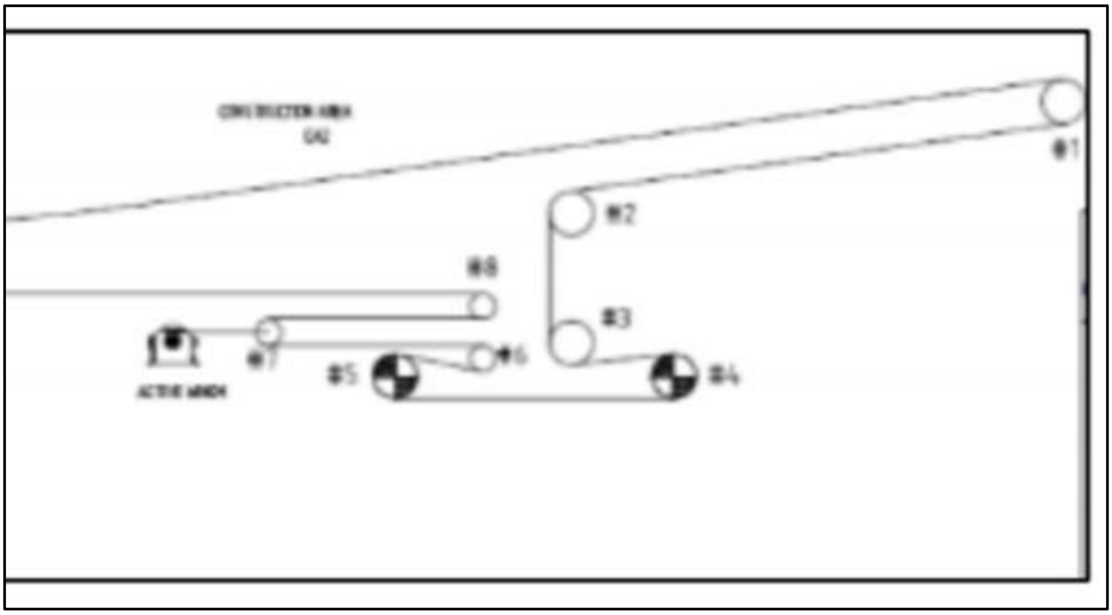

Figure 12 – An example of a tandem drive.

Before digital controllers existed, the standard practice in tandem drives was to use a fluid coupling connection between the motor and the pulley on one of the drives to allow for the inability to precisely attain synchronous speeds, at the expense of some power loss. Conveniently, it allowed for slightly asynchronous speed and the drives ran smoothly. As greater efficiency has been pursued, the fluid coupling has been replaced by electronics that allow precise matching of dual drive speeds. The assumption is matched speeds would maximise efficiency and minimise wear, but instead, persistent pulsations occur and lagging wear is accelerated. Greater speed accuracy is pursued, yet this does not solve the problem. The irony is the rubber materials used to drive the belt have viscoelastic traits that require a slight speed difference. At synchronous speeds, the second drive experiences repeated micro breakaway events because the generated friction coefficient is slip deficient to prevent the belt from breaking away. But as it begins breakaway, the extra slip generates the needed friction and stops the breakaway. However, now there is insufficient ongoing slip to generate the needed friction and the process is repeated.

CONCLUSION

Lagging friction defies a simple description. It is not merely an easy coefficient to be used in the capstan equation. The data presented shows there is an irreducible link between lagging creep history and generated friction coefficient. One cannot be calculated without the other. Nevertheless, with the equations presented in this paper it is now possible to accurately predict both behaviours through an iterative calculation. Optimisation of drive efficiency, lagging stress, and resultant wear is available at the design stage of conveyor engineering.

For existing drives, the calculations allow for proper lagging selection by minimising creep at an acceptable cost. Creep can be reduced with higher modulus belts, smaller tension ratios, or with a different lagging technology. Under the right circumstances, a more costly lagging option can reduce the overall creep to acceptable levels. On the other hand, the choice to replace a steel corded belt with a ply belt of the same rating could be analysed for possible lagging issues.

One interesting outcome of this analysis has been the relative unimportance of lagging thickness. Experiments with the calculator show relatively little change in the lagging performance. If anything, the lagging slip necessary to sustain the T1/T2 ratio increases slightly. The primary benefit of increased thickness lies in the ability to cushion the effects of uneven tension profiles across the belt width. A thick lagging can compress to a greater degree under extra wrap pressure and change the diameter the belt must traverses around the pulley to help smooth the tension profile.

REFERENCES

1 DeVries, B. (2015). Varient Lagging Friction Coefficents and Implications. IMHC Beltcon 18

2 Bowden, F., & Tabor, D. (1939). The area of contact between stationary and between moving surfaces. *Proc. R. Soc. A, 169*, 391-413.

3 Persson, B. (1998). On the theory of rubber friction. *Surface Science, 401*, 445-454.

4 DeVries, B. (2017). Surface Dynamics of Belt Conveyor Pulleys. IMHC Beltcon 19

5 Perrson, B. (2011). Rubber friction and tire dynamics. J. Phys,: Condens. Matter **23**, 015003

ABOUT THE AUTHORS

BRETT DEVRIES

Mr. Brett DeVries is a Staff HD Product Development Engineer with 24 years of employment with Flexible Steel Lacing Company (FLEXCO), a US-based multinational company specialising in maximising belt conveyor productivity. Mr. DeVries holds a Bachelor of Science in Mechanical Engineering degree from Calvin University in Grand Rapids, Michigan and is a registered Professional Engineer by the State of Michigan. Mr. DeVries holds 30+ US and international patents and is an active member in Conveyor Equipment Manufacturers Association (CEMA) and the Society for Mining, Metallurgy & Exploration (SME).

Brett DeVries

Flexible Steel Lacing Company

1854 Northridge Dr. NW

Walker, MI USA

+1 616 459-3196

bdevries@flexco.com